

X-RAY SOURCES WITH PERIODIC VARIABILITY IN A DEEP *Chandra* IMAGE OF THE GALACTIC CENTERM. P. MUÑO,<sup>1</sup> F. K. BAGANOFF,<sup>1</sup> M. W. BAUTZ,<sup>1</sup> W. N. BRANDT,<sup>2</sup> G. P. GARMIRE,<sup>2</sup> AND G. R. RICKER<sup>1</sup>*Draft version November 22, 2018*

## ABSTRACT

We report the discovery of eight X-ray sources with periodic variability in 487 ks of observations of the Galactic center with *Chandra*. The sources are identified from a sample of 285 objects detected with 100–4200 net counts. Their periods range from 300 s to 4.5 h with amplitudes between 40% and 70% rms. They have luminosities of  $(1 - 5) \times 10^{32}$  erg s<sup>-1</sup> (2–8 keV at 8 kpc). The spectra of seven of the eight sources are consistent with  $\Gamma \approx 0$  power laws absorbed by gas and dust with a column density equal to or higher than that toward the Galactic Center ( $6 \times 10^{22}$  cm<sup>-2</sup>). Four of these sources also exhibit emission lines near 6.7 keV from He-like Fe, with equivalent widths of 600–1000 eV. These properties are consistent with both magnetically accreting cataclysmic variables and wind-accreting neutron stars in high-mass X-ray binaries. The eighth source has an absorbing column of  $5 \times 10^{21}$  cm<sup>-2</sup> that places it in the foreground. Its spectrum is consistent with either a  $\Gamma = 1.4$  power law or  $kT = 25$  keV bremsstrahlung emission. Its period-folded flux profile clearly identifies it as an eclipsing polar. We place an approximate upper limit of  $i' > 23$  magnitude on the optical counterpart to this source using a 5 min exposure obtained with the MagIC camera on the Clay telescope (Magellan II) at Las Campañas.

*Subject headings:* X-rays: binaries — stars: rotation — stars: pulsars — stars: cataclysmic variables

## 1. INTRODUCTION

In order to understand the star-formation history of our Galaxy, it is important to know the numbers of stars that have long since ended their lives on the main sequence. Although the compact remnants of dead stars — white dwarfs, neutron stars, and black holes — are generally difficult to find in isolation, they can be identified relatively easily if they are accreting significant amounts of matter from a companion star in a close binary orbit. As the matter falls in toward the compact object, it is heated and shocked, causing it to emit  $10^{29}$ – $10^{39}$  erg s<sup>-1</sup> of X-rays (see Warner 1995; White, Nagase, & Parmar 1995, for reviews). When combined with sophisticated models for the evolution of these close binaries, the observed numbers of accreting X-ray sources can provide estimates of the total numbers of black holes, neutron stars, and white dwarfs in the Galaxy (Iben, Tutukov, & Fedorva 1997; Kalogera 1999; Howell, Nelson, & Rappaport 2001; Podsiadlowski, Rappaport, & Pfahl 2002).

Such a study could be particularly fruitful toward the Galactic center, where the star-formation history is uncertain (Morris 1993; Serabyn & Morris 1996) and the stellar density is high enough that it is possible to assemble a statistically meaningful sample of X-ray sources from a relatively small field. We have recently carried out a census of X-ray emitting objects brighter than 10<sup>30</sup> erg s<sup>-1</sup> in a 17' by 17' field around Sgr A\* using the *Chandra X-ray Observatory* (Muñoz et al. 2003). We detected over 2300 individual point sources in this field, the natures of most of which are unknown because a wide range of stellar systems emit X-rays at this level. However, more than half of the 800 sources that were bright enough to provide spectral information ( $\gtrsim 60$  net counts above 2 keV) had

very hard spectra, consistent with a power law  $E^{-\Gamma}$  with photon index  $\Gamma < 1$ . Such hard spectra have only been observed previously from two classes of source: neutron stars accreting from the winds of young, massive companions (high-mass X-ray binaries, or HMXBs, most of which are X-ray pulsars; see Apparao 1994; Campana et al. 2001), and old, magnetically-accreting white dwarfs (polars and intermediate polars; see Ezuka & Ishida 1999).

In both classes of source, the compact object has a strong magnetic field that channels accreted material onto polar caps. If the field is mis-aligned with the spin axis of the compact object, then the caps can produce modulated X-ray emission. The amplitudes of the pulsed emission from pulsars and polars can be more than 40% rms (e.g., Haberl et al. 1998; Reig & Roche 1999; Norton & Watson 1989). Therefore, in order to explore the natures of the hard X-ray sources at the Galactic center, we have searched for periodic X-ray variability during a 487-ks exposure that was taken over the course of two weeks in 2002 May to June. In this paper, we report the detection of eight sources that exhibit periodic X-ray variability in the direction of the Galactic center. We discuss their natures based upon the lengths of their periods and the spectral properties of their X-ray emission. We also report an upper limit on the optical magnitude of one X-ray source with periodic variability that lies in the foreground of the Galactic center.

## 2. OBSERVATIONS AND DATA ANALYSIS

Twelve separate pointings toward the Galactic center have been carried out using the Advanced CCD Imaging Spectrometer imaging array (ACIS-I; Garmire et al. 2002) aboard the *Chandra X-ray Observatory*, in order to monitor Sgr A\* (Table 1). The ACIS-I is a set of four 1024-

<sup>1</sup> Center for Space Research, Massachusetts Institute of Technology, Cambridge, MA 02139; muñoz@space.mit.edu, fkb@space.mit.edu<sup>2</sup> Department of Astronomy and Astrophysics, The Pennsylvania State University, University Park, PA 16802

by-1024 pixel CCDs, covering a field of view of  $17' \times 17'$ . When placed on-axis at the focal plane of the grazing-incidence X-ray mirrors, the imaging resolution is determined primarily by the pixel size of the CCDs,  $0''.492$ . The CCDs also measure the energies of incident photons, with a resolution of 50–300 eV (depending on photon energy and distance from the read-out node) within a calibrated energy band of 0.5–8 keV. The CCD frames are read out every 3.2 s, which provides the nominal time resolution of the data.

The methods we used to create a combined image of the field, to identify point sources, and to compute the photometry for each source are described in Muno et al. (2003). In brief, we created an event list for each observation in which we corrected the pulse heights of each event for the position-dependent charge-transfer inefficiency (Townsley et al. 2000). We excluded non-X-ray background events, events that did not pass the standard ASCA grade filters and CXC good-time filters, and intervals of strong background flaring. We used the CIAO tool `acis_bary` to correct the arrival time of each event to the Solar System barycenter. The final total live time was 626 ks. We then applied a correction to the absolute astrometry of each pointing using three Tycho sources detected strongly in each *Chandra* observation (see Baganoff et al. 2003), and re-projected the sky coordinates of each event to the tangent plane at the radio position of Sgr A\* in order to produce a single composite image. The image (excluding the first part of ObsID 1561, during which a  $10^{-10}$  erg cm $^{-2}$  s $^{-1}$  transient was observed) was searched for point sources using `wavdetect` in three energy bands (0.5–8 keV, 0.5–1.5 keV, and 4–8 keV) using a significance threshold of  $10^{-7}$ . We detected a total of 2357 X-ray point sources, of which 1792 were detected in the full band, 281 in the soft band (124 exclusively in the soft band), and 1832 in the hard band (441 exclusively in the hard band).

We computed photometry for each source in the 0.5–8.0 keV band using the `acis_extract` routine (Broos et al. 2002) from the Tools for ACIS Real-Time Analysis (TARA).<sup>3</sup> We extracted event lists for each source for each observation, using a polygonal region generally chosen to match the contour of 90% encircled energy from the PSF, although smaller regions were used if two sources were nearby in the field. We used a PSF at the fiducial energy of 1.5 keV for foreground sources, while we used a larger extraction area corresponding to an energy of 4.5 keV for Galactic center sources. A background event list was extracted for each source from a circular region centered on the point source, excluding from the event list (i) counts in circles circumscribing the 95% contour of the PSF around any point sources and (ii) bright, filamentary structures. The size of each background region was chosen such that it contained  $\approx 1200$  total events for the 12 observations. The net counts in each energy band were computed from the total counts in the source region minus the estimated background. The photometry for the complete sample of sources is listed in the electronic version of Table 3 from Muno et al. (2003).

## 2.1. Periodicity Search

<sup>3</sup> <http://www.astro.psu.edu/xray/docs/TARA/>

We searched for periodicities using data from the 487 ks of observations that took place over 14 days between 2002 May 22 and June 4 (Table 1). These observations are long enough to provide good signal-to-noise, and they occur over a short enough amount of time that a single ephemeris is likely to be applicable to a signal from any given source (although see Section 3). We searched all 285 sources with more than 100 net counts during this time interval. We did not search for periodicities in the remaining 139 ks of data, which were taken in 11–41 ks exposures separated by up to a year. It is not possible to identify periods in the individual observations because the sources are too faint, and combining all of the observations would require a prohibitively large search through the parameter space of possible ephemerides.

We produced a periodogram of each source using the  $Z_1^2$  or Rayleigh statistic (Buccheri et al. 1983),

$$Z_1^2 = \frac{2}{N} \sum_j (\cos^2 \phi(t_j) + \sin^2 \phi(t_j)), \quad (1)$$

where  $N$  is the total number of events,  $t_j$  is the arrival time of an event, and  $\phi$  is the phase at time  $t$  that would be expected for a constant-frequency modulation  $\phi(t) = 2\pi\nu t$ . The lowest frequency ( $\nu$ ) considered was  $1 \times 10^{-5}$  Hz, which is approximately the inverse of the length of the longest observation. The highest frequency was 0.1 Hz, as the photon arrival times are only recorded with an accuracy of 3.2 s. The frequency resolution was  $1 \times 10^{-6}$  Hz, which is the inverse of the total time, 10<sup>6</sup> s spanned by the observations used to search for periodicities. This is the highest resolution with which the periodogram can be sampled using independent frequency bins. For a signal resulting purely from Poisson noise (i.e., a white-noise signal),  $Z_1^2$  has a chi-squared distribution with two degrees of freedom. This statistic is useful in a case like ours when the arrival times of individual photons are well-known, and yet there are too few photons to analyze evenly-binned data. This method also naturally ignores gaps in the data produced when the Galactic center was not observed. We performed Monte-Carlo simulations that indicate that these gaps do not cause significant noise leakage due to the sampling window function (see Press et al. 1992 pp. 437–447 for a general discussion of noise leakage). Red noise due to long term variability is apparent below  $5 \times 10^{-5}$  Hz in the power spectra of  $\approx 10\%$  of the sources, but does not otherwise affect the detectability of coherent signals at higher frequencies.

Each of the 285 sources was searched for periodicities in approximately  $\approx 10^5$  frequency bins, so  $3 \times 10^7$  trial frequencies were examined in total. Therefore, there is only a 1% chance that Poisson noise would produce a signal stronger than  $Z_1^2 > 43.5$  in our entire search. We consider any signal stronger than this to be a secure detection of a periodicity. The rms amplitude  $A$  of a sinusoidal signal can be computed from  $Z_1^2$  as

$$A = \left( \frac{Z_1^2}{N} \right)^{1/2} \frac{N}{N - B}, \quad (2)$$

where  $N$  is the total number of events from the extraction region, and  $B$  is the number of background counts (e.g., Leahy et al. 1983). Given the typical background of 30

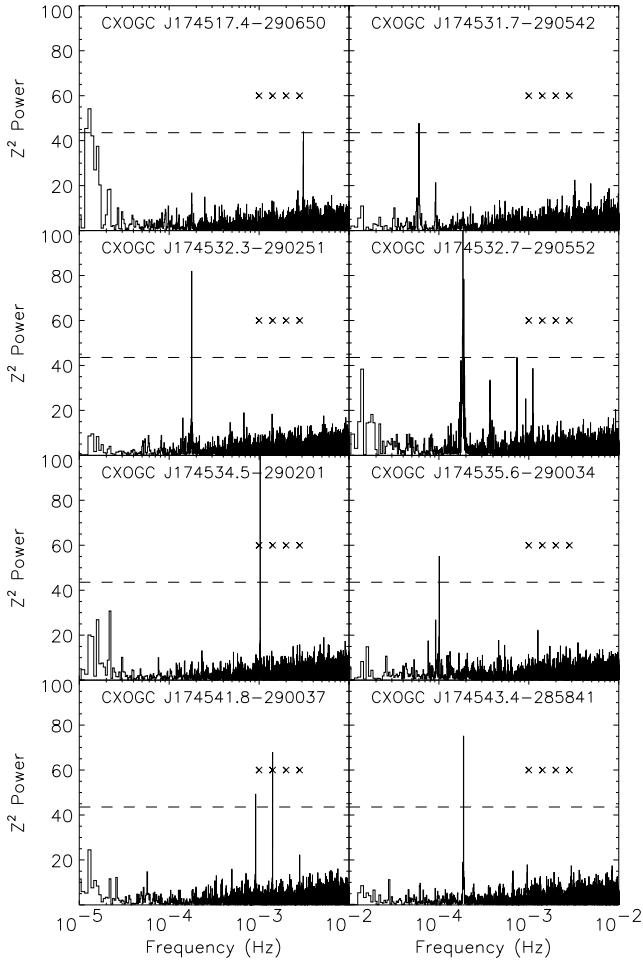


FIG. 1.— Periodograms of the eight sources in which significant periodicities are detected, computed using the  $Z_1^2$  statistic. We have only plotted frequencies between  $10^{-5}$  and  $10^{-2}$  Hz, since between  $10^{-2}$  and  $10^{-1}$  the power is dominated by noise. The dashed lines indicate the 99% confidence level for detecting a signal given the total number of sources and frequency bins searched. The x's indicate frequencies at which spurious signals from the satellite dither would be expected if the source were near a chip gap or bad column. CXOGC J174541.8-290037 exhibits a signal at the pitch frequency of  $1.415 \times 10^{-3}$  Hz, in addition to the intrinsic signal at  $9.16 \times 10^{-4}$  Hz.

counts for a source within a few arcminutes of the aim-point, we would be able to detect a completely modulated signal (70% rms) with only 100 counts from a source.

We detected 23 significant periodicities. We then checked to ensure that none of them were at multiples of the frequencies at which the pointing of the satellite is dithered. The dither is designed to distribute photons over many CCD pixels, and has a period of 706.96 s in pitch and 999.96 s in yaw. The count rate from a source that lies near a chip gap or bad column would appear to vary with one or both of the above periods. There were 16 sources that exhibited variations at multiples of the dither frequencies, all of which lay near chip gaps or bad columns. Significant periodicities that were clearly not associated with the dither frequencies were detected from 8 sources (including one that also exhibited variations at a dither frequency). The locations of these sources on the ACIS-I CCDs did not suggest any instrumental anomalies

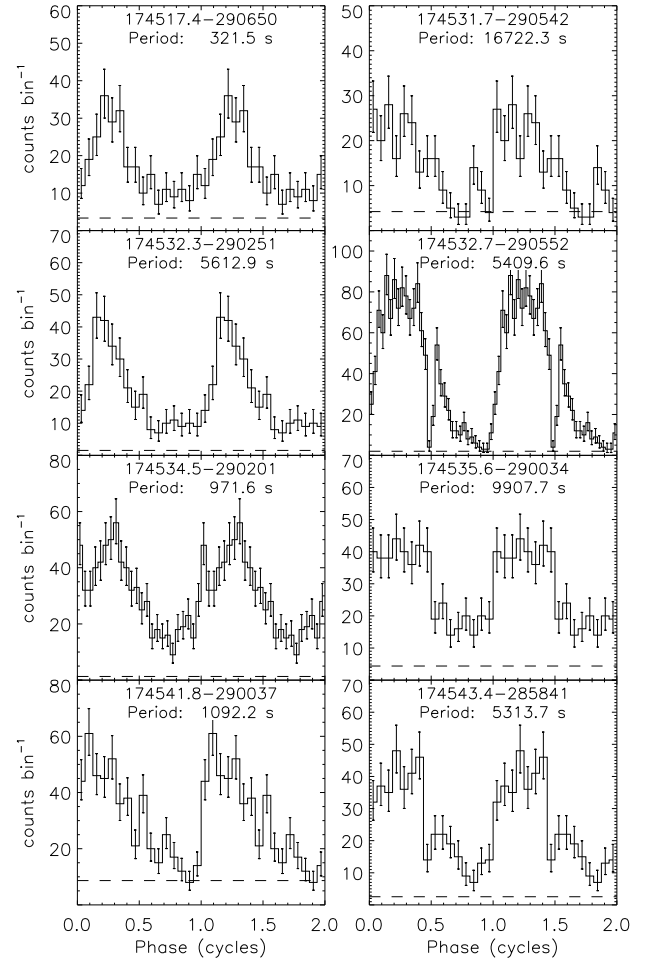


FIG. 2.— Folded profiles of the eight sources with significant X-ray periodicity, repeated for two cycles for clarity. The background level is indicated with a dashed line. CXOGC J174517.4-290650, CXOGC J174532.3-290251, and CXOGC J174532.7-290552 exhibit significant harmonic content, while the profiles of the remaining sources are consistent with sinusoids. The uncertainties are  $1\sigma$  upper and lower bounds defined according to Gehrels (1986).

that might produce periodicities, so we concluded that the periods are intrinsic to the sources themselves. We listed these eight sources in Table 2, and displayed their power spectra in Figure 1.

We found possible periodicities in three more sources, but these require further confirmation to be considered secure. Two sources appear to produce highly significant coherent signals at very low frequencies: CXOGC J174540.1-290055 ( $1.5 \times 10^{-5}$  Hz), and CXOGC J174552.2-290744 ( $1.4 \times 10^{-5}$  Hz). Although the power appears to be strongly peaked at the above frequencies, and there is little power elsewhere below  $5 \times 10^{-5}$  Hz, it cannot be ruled out that these periodicities result from red noise. Moreover, the periods are so long that fewer than 3 cycles could be detected in the longest individual observation. The third source, CXOGC J174546.2-285906, exhibits a coherent signal at  $6 \times 10^{-5}$  Hz with  $Z_1^2 = 37.7$ . This signal has an 18% chance of occurring due to Poisson noise given our entire search, so we do not include it with the secure detections in Table 2. Unfortu-

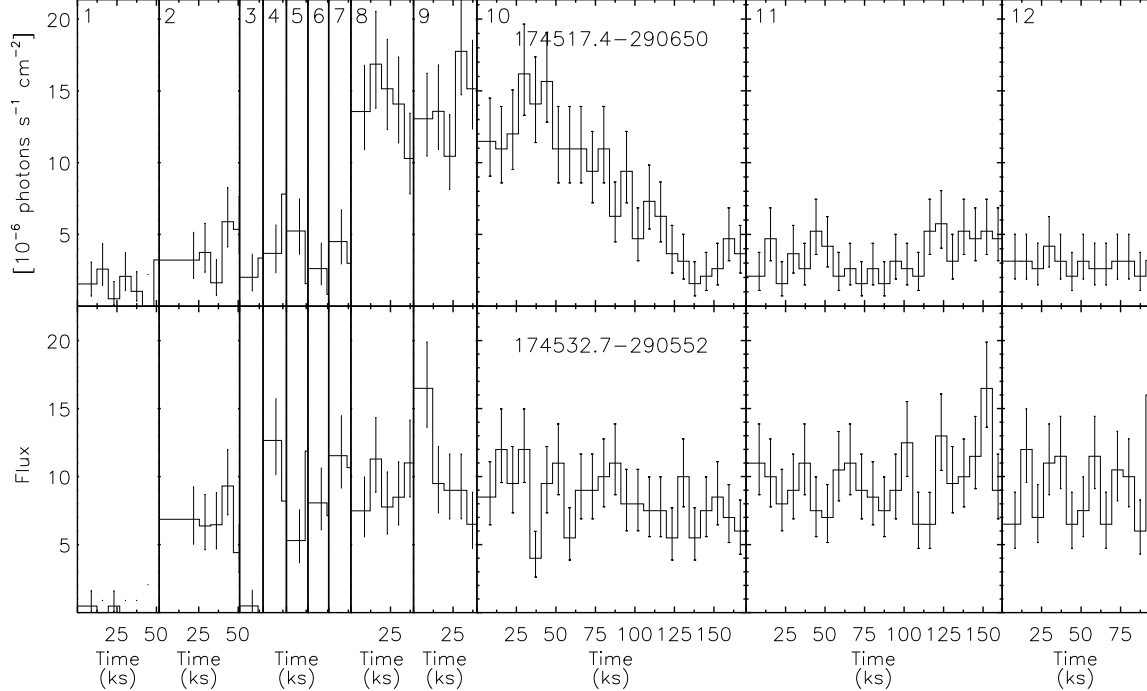


FIG. 3.— Photon fluxes from the two sources that exhibit significant long-term variability, computed by dividing the count rate by the mean value of the ARF and by the exposure in each bin. The background level has not been subtracted. Data from the individual observations are plotted in 7200-s bins in order to illustrate the short-term variability; the number of each observation from Table 1 is indicated at the top. The total time over which the data were taken spans nearly three years. The flare from CXOGC J174517.4–290650 was visible for three weeks. The energy flux can be estimated by assuming the spectrum is a  $\Gamma = 0.5$  power law absorbed by a column of  $6 \times 10^{22} \text{ cm}^{-2}$ , for which the mean energy per photon is  $8 \times 10^{-9} \text{ erg}$  (2–8 keV). The uncertainties are  $1\sigma$  upper and lower bounds defined according to Gehrels (1986).

nately, the remaining observations (1–7 in Table 1) did not provide enough counts to confirm these possible signals.

In order to determine the period of the variability for each source in Table 1 more accurately, we computed  $Z_1^2$  over a frequency range of  $2 \times 10^{-6}$  Hz around the peak power in the periodogram using a frequency resolution of  $10^{-7}$  Hz. This over-samples the frequency resolution for which each measurement of the power is independent by a factor of 10, allowing us to precisely determine the frequency at which the largest power is produced. The corresponding periods are listed in Table 2. We then produced light-curves folded at the period obtained from the peak of the over-sampled periodogram, which are displayed in Figure 2. We measured the amplitudes and ephemerides of the periodicities by fitting a sine function to the folded profile, and listed these quantities in Table 2. Therefore, the amplitude is that of the fundamental sinusoidal component of the variation, which is useful for comparison to amplitudes and upper limits detected in periodicity searches. The ephemeris is defined by the zero phase of the sine function closest to the start of the observation, and is reported in Modified Julian Days, Barycentric Dynamical Time. We determined the  $1\sigma$  uncertainties on the parameters listed in Table 2 using a Monte-Carlo simulation, in which we produced 100 light curves that matched the measured count rate, sampling window, and period and amplitude of the sinusoidal signal for the data from each source, and analyzed them in the same manner as the real events.

We next characterized the shapes of the modulations by computing Fourier power spectra of the folded pro-

files from each source in Figure 2. Power at the first harmonic of the main signal was present in CXOGC J174517.4–290650 and CXOGC J174532.3–290251 with a single-trial probability of 0.7% that they were due to noise (power  $p = 10$  using the normalization of Leahy et al. 1983), and from CXOGC J174532.7–290552 with a single-trial chance probability of  $10^{-11}$  ( $p = 50$ ). The harmonic signals from the other sources had a single-trial probability of at least 5% that they were due to noise. We converted the powers of the harmonic signals to fractional rms amplitudes using Equation 2, substituting the Fourier power for  $Z_1^2$  (Leahy et al. 1983). We also computed  $1\sigma$  uncertainties on the amplitudes, taking into account the expected distribution of power from Poisson noise (Vaughan et al. 1994). In all three cases, the first harmonics had a rms amplitudes of  $20\% \pm 5\%$ . We found no evidence for higher harmonics. We also folded the data about  $1/2$  the period of the strongest signal in order to search for evidence that the main signals are produced by two magnetic poles on the compact object. Marginally significant power was detected at half the period of the main signal only from CXOGC J174535.6–290034, with a 2% chance that it was due to Poisson noise for a single trial ( $p = 7$ ).

We also searched for energy dependence in the amplitudes and shapes of the pulse profiles. We derived folded profiles for each source in the 0.5–4.7 keV and 4.7–8.0 keV bands, and computed Fourier power spectra of the resulting profiles to quantify their amplitudes and harmonic content. We find that the pulse profiles from three sources are inconsistent with a constant amplitude at the  $2.5\sigma$  level. The modulation amplitudes decrease with energy in CX-

OGC J174517.4–290650 from  $(74 \pm 11)\%$  to  $(36\% \pm 9)\%$ , and in CXOGC J174543.4–285841 from  $(62 \pm 9)\%$  to  $(34 \pm 6)\%$  (uncertainties are  $1\sigma$ ). The modulation amplitude increases with energy in CXOGC J174541.8–290037 from  $(29 \pm 7)\%$  to  $(53 \pm 6)\%$ . Given that the profiles of these three systems contain only 100–200 net counts in each energy band, it would be useful to confirm these results with future observations. The amplitudes of the variations for the other sources were constant with energy to within their  $1\sigma$  uncertainties. We find no evidence for changes in the shapes of the profiles as a function of energy.

Finally, in order to search for variability in each source aside from the periodic signals, we extracted light curves using the CIAO tool `lightcurve`. Two sources exhibited long-term X-ray variability, so we display them in Figure 3. One of the two, CXOGC J174532.7–290552, appears fainter in the observations in 1999 September (ObsID 0242) and 2001 July (ObsID 1561, part 2) than in the remaining observations, but its mean flux was constant during the observations in 2002 May and June. The other, CXOGC J174517.4–290650, decreased from a flux of  $9 \times 10^{-14}$  erg cm $^{-2}$  s $^{-1}$  to  $8 \times 10^{-15}$  erg cm $^{-2}$  s $^{-1}$  during ObsID 3392 (we have assumed a  $\Gamma = 0.5$  power law absorbed and scattered by  $N_{\text{H}} = 6 \times 10^{22}$  cm $^{-2}$  of gas and dust). We searched for pulsations from this source separately in the first two and last two observations, when the mean flux from the source did not vary strongly. The pulsations are detected strongly in ObsIDs 2943 and 3663, and their properties are listed in Table 2. The oscillations are not detectable in ObsIDs 3393 and 3665 due to the low count rate; with only 77 net events from the source against 140 background events, a fully modulated sinusoidal signal would be undetectable (Equation 2).

## 2.2. Spectra

In order to compare the Galactic center sources with periodic X-ray variability to known classes of objects, we extracted their phase-averaged energy spectra from the entire 626 ks data set. We computed the effective area function (ARF) at the position of each source for each observation. This was corrected to account for the fraction of the PSF enclosed by the extraction region and for the variable hydrocarbon build-up on the detectors.<sup>4</sup> We used response matrices appropriate for data corrected to account for charge-transfer inefficiency. We used the average of the effective area and response functions, weighted by the number of counts from each source in each observation.

We modeled the X-ray spectra in `XSPEC`, using a power-law continuum absorbed at low energies by gas (using the model `phabs` in `XSPEC`) and dust (using a modified version of the model `dust` in which the approximation that the dust was optically thin was removed). The column depth of dust was set to  $\tau = 0.485 \cdot N_{\text{H}} / (10^{22} \text{ cm}^{-2})$  (Baganoff et al. 2003), and the halo size to 100 times the PSF size. The spectra with the resulting fits are displayed in Figure 4. Half of the sources could not be adequately fit with this simple model; from Figure 4 it is clear that this is at least partly due to excess counts between 6–7 keV, where one expects emission from both neutral and highly-ionized iron. Therefore, we added Gaussian lines

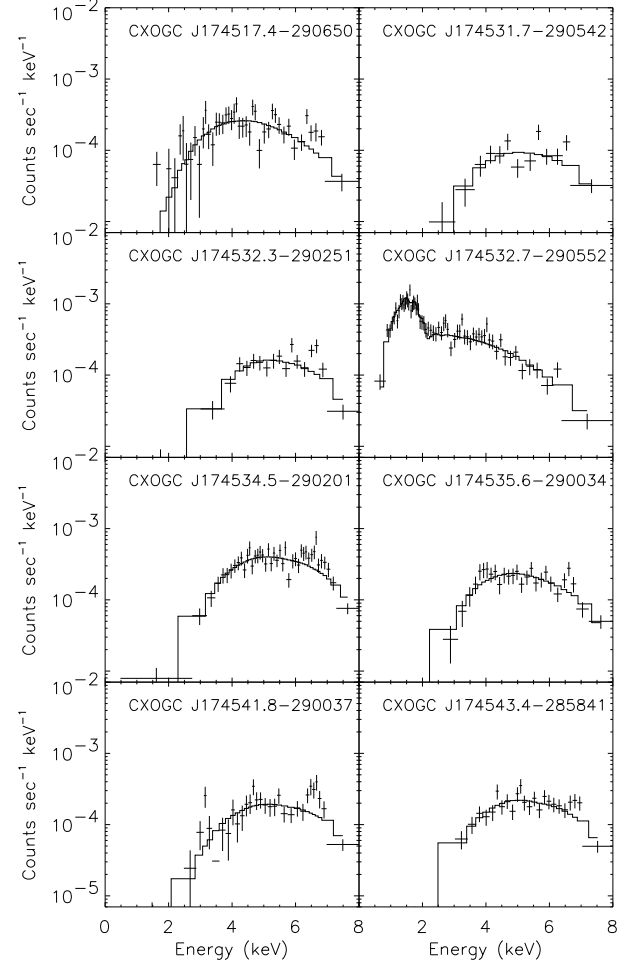


FIG. 4.— X-ray spectra of the eight sources with periodic X-ray variability. Each spectrum is displayed in units of detector counts  $\text{s}^{-1} \text{ keV}^{-1}$  as a function of energy in keV, so that the varying effective area of the detector is convolved with the spectrum. The solid histograms represent the best-fit absorbed power laws. The power laws are statistically acceptable in four cases, while in the remaining four there are significant residuals near 6.7 keV, where emission from highly ionized iron is expected (see Table 3). CXOGC J174532.7–290552 is in the foreground of the Galactic center, as evident from the copious emission below 2 keV. The remaining sources lie near or beyond the Galactic center, and exhibit hard ( $\Gamma < 1$ ) power laws.

to the models for these four sources, which significantly improved the fits. The resulting spectral parameters are listed in Table 3.

The column of gas and dust toward all but one of the sources is comparable to or greater than the value toward Sgr A\*,  $6 \times 10^{22} \text{ cm}^{-2}$  (Baganoff et al. 2003). The remaining source, CXOGC J174532.7–290552, is clearly located in the foreground of the Galactic center. This source also has the softest spectrum, which is consistent with either a  $\Gamma = 1.4$  power law or a  $kT = 25$  keV bremsstrahlung continuum. The remaining sources either have hard X-ray spectra that are consistent with  $\Gamma < 1$  power laws, or have poorly constrained  $\Gamma \sim 0 - 2$  continuum spectra with evidence for Fe emission lines. If we use a bremsstrahlung

<sup>4</sup> [http://cxc.harvard.edu/cal/Acis/Cal\\_prods/qeDeg/](http://cxc.harvard.edu/cal/Acis/Cal_prods/qeDeg/)

continuum spectrum instead, we only obtain lower limits on their temperatures of about 30 keV. We note that this does not necessarily imply that the spectra are intrinsically that flat. Given that the absorbing columns toward several of the sources are larger than the Galactic value, it is possible that absorbing material local to each of these sources partially covers the X-ray emitting regions (compare Apparao et al. 1994; Ezuka & Ishida 1999). This can make a spectrum look much flatter than it is intrinsically. Such a “partial-covering absorber” model is often used for magnetic CVs, but we feel that using this more complicated model for the current data is unwarranted given the small number of counts recorded for each source.

Emission lines from Fe are present in at least four of the Galactic center sources with periodic variability (Table 3). The equivalent widths of the lines range from 600–1000 eV for the sources for which an absorbed power law alone cannot adequately model the spectrum. The lines are all located at approximately 6.7 keV, indicating that they result from He-like Fe. Likewise, if we add a Gaussian line at  $\approx 6.7$  keV to those Galactic center sources for which an absorbed power law does provide an adequate fit, we find that their best-fit equivalent widths are 400–700 eV. Although the equivalent widths of these lines are similar to those observed from the diffuse X-ray emission from the Galactic center (Park et al., in preparation), the construction of the background regions ensures that the line emission originates from the point sources. We have also confirmed that each of the sources with strong 6.7 keV emission is visible as a point source in an image produced from 6.5–7.0 keV X-rays. On the other hand, any ionized Fe emission from the foreground source CXOGC J174532.7–290552 must be weak, as the 90% upper limit on the equivalent width of a line at 6.7 keV is 100 eV.

The lines detected from the Galactic center sources were resolved with widths of 0.14–0.3 keV in three out of four cases. Several factors could contribute to the width of the lines: they could be a blend of several ionization species, Doppler-broadened by the motions of the accreted material, or broadened by Compton scattering in the accretion flow (e.g., Hellier, Mukai, & Osborne 1998).

### 3. DISCUSSION

We have searched for periodicities in 285 sources detected with more than 100 net counts during 487 ks of *Chandra* observations of the Galactic center taken from 2002 May 22 to June 4. In eight of these sources, we have found significant variability with periods ranging from 320 s to 4.5 h and amplitudes ranging from 40–70% rms. Our search for pulsations was motivated by the prevalence of sources with hard ( $\Gamma < 1$ ) power-law spectra in the *Chandra* image of the Galactic center, which we have tentatively identified as either magnetically-accreting white dwarfs or wind-accreting neutron stars (Muno et al. 2003; see also Apparao 1994; Ezuka & Ishida 1999). We have illustrated which of the sources are observed with periodicities in Figure 5, in which we plot the net number of counts (0.5–8.0 keV) from each source versus a hard color that parameterizes the steepness of the spectrum. The hard color is defined as  $(h - l)/(h + l)$ , where  $h$  is the number of counts from 4.7–8.0 keV and  $l$  is the number of counts

from 3.3–4.7 keV. Not surprisingly, the brightest sources are more likely to be detected with periodicities, since the minimum detectable pulsed fraction decreases as the net number of counts from a source increases (Equation 2). Moreover, seven of the sources with periodic variability have hard colors  $> 0$  (Fig. 5), which are consistent with  $\Gamma < 1$  power-law spectra (Table 3 and Figure 4). This supports the suggestion that many of the hard sources are either magnetic CVs or HMXB pulsars. These seven sources also are heavily absorbed, which suggests that they are located at or beyond the Galactic center (Table 3). The eighth source is a relatively soft foreground source, and will be discussed in detail in Section 3.2.

#### 3.1. The Natures of the Galactic Center Sources

It is difficult to determine whether the Galactic center systems with periodicities are magnetic CVs or HMXB pulsars based on the X-ray data alone. The luminosities of the Galactic center sources range from  $(1 - 5) \times 10^{32}$  erg s $^{-1}$  (2–8 keV at 8 kpc). These luminosities are comparable to those of the brightest observed magnetic CVs (Verbunt et al. 1997; Ezuka & Ishida 1999; Grindlay et al. 2001; Pooley et al. 2002), but are a factor of  $\approx 10$  below the luminosities of the faintest known HMXB pulsars (Negueruela et al. 2000; Campana et al. 2001). However, HMXBs are less common in the Galaxy than magnetic CVs (compare Pfahl, Rappaport, & Podsiadlowski 2002; Howell et al. 2001), and most HMXBs are identified through transient outbursts that reach luminosities of 10 $^{38}$  erg s $^{-1}$ . Therefore, the known HMXBs lie at much greater distances than the known CVs — the typical distance for an HMXB is  $\sim 8$  kpc, compared to  $\sim 100$  pc for a magnetic CV (Apparao et al. 1994; Warner 1995). The lack of known HMXBs with low luminosities may be a selection effect, and the hard Galactic center sources could represent the first such systems identified (Pfahl et al. 2002).

The spectra of magnetic CVs and HMXB pulsars also can appear similar between 2–8 keV. Both types of systems can often be described with a  $\Gamma < 1$  power-law continuum, and both exhibit iron emission between 6–7 keV with equivalent widths up to  $\sim 500$  eV (Apparao et al. 1994; Hellier et al. 1998; Ezuka & Ishida 1999). The Fe emission from three of the Galactic center sources also appears to be resolved (Table 3). Likewise, Fe emission was resolved with widths of  $\sim 200$  eV from about half of the magnetic CVs studied using the *ASCA* SIS by Hellier et al. (1998). To our knowledge, 6.7 keV Fe lines this broad have not been reported from HMXB pulsars, although this may be because few comparable studies of the Fe lines from such systems have been carried out using CCD-quality spectra.

The properties of the modulations observed from the Galactic center sources suggest that they originate from the spin periods of either magnetically-accreting white dwarfs or wind-accreting neutron stars. The modulation amplitudes in Table 2 range from 40% to 70% rms. Similarly, a survey of the literature yields a range of 5–40% rms for the amplitudes of pulsations from magnetic CVs (e.g., Norton & Watson 1989; Schwarz et al. 2002; Ramsay & Cropper 2003), and 5–50% rms for HMXB pulsars (Rappaport & van den Heuvel 1982; Haberl et al. 1998; Reig & Roche 1999; Israel et al. 2000; Hall et al. 2000). We have also detected significant non-sinusoidal components

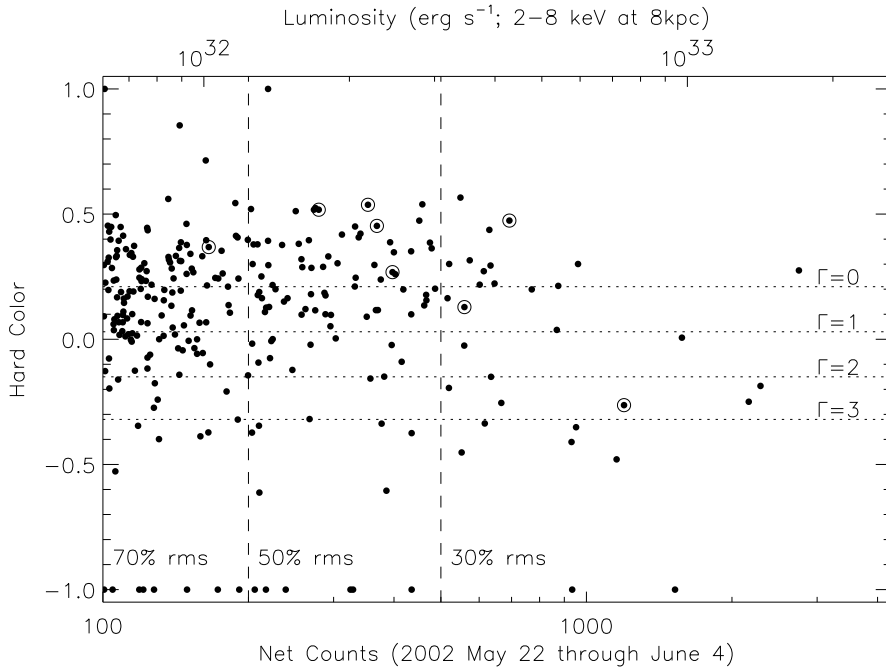


FIG. 5.— Hard colors of the 285 sources searched for periodicities plotted as a function of the net counts (0.5–8.0 keV) from each source during the 7 observations taken between 2002 May 22 and June 03. The hard color is defined as  $(h - l)/(h + l)$ , where  $h$  is the number of counts from 4.7–8.0 keV and  $l$  is the number of counts from 3.3–4.7 keV. The luminosities of the sources are indicated by the axis at the top of the figure, where we have assumed 1 count/487 ks =  $8 \times 10^{-17}$  erg cm $^{-2}$  s $^{-1}$  and a distance of 8 kpc. The conversion was computed using PIMMS for a  $\Gamma = 0.5$  power-law spectrum absorbed by  $6 \times 10^{22}$  cm $^{-2}$  of gas and dust. It is only approximate because it does not take into account vignetting or the dither in the satellite pointing. The vertical dashed lines indicate the numbers of net counts needed to detect a modulation with fractional rms amplitude of 50% and 30% on top of 30 counts of background; a fully modulated signal (70% rms) can just be detected from the sources with 100 net counts in this diagram. The horizontal dotted lines indicate the hard colors corresponding to power-law spectra over a range of photon index  $\Gamma$ , assuming an absorption column of  $6 \times 10^{22}$  cm $^{-2}$ . Sources above the  $\Gamma = 1$  line are likely to be magnetized CVs or HMXB pulsars located at the Galactic center. Sources with detected periodicities are marked additionally with open circles, in order to convey the fraction of hard sources that are detected with oscillations as well as the number of sources in which oscillations of a given amplitude could have been detected.

in the profiles of three sources in Figure 2 (see Section 2.1), which is commonly seen from both HMXB pulsars and magnetic CVs (e.g., Rappaport & van den Heuvel 1982; Ramsay & Cropper 2003). Unfortunately, aside from in CXOGC J174532.7–290552 (see Section 3.1), there is not enough signal from the Galactic center sources to speculate in detail on how the pulse shape is formed.

The periods of the modulations are also consistent with the spin periods of white dwarfs in CVs and neutron stars in HMXBs. The median spin period of the 112 magnetic CVs in the catalog of Ritter & Kolb (2003) is  $P \approx 6000$  s. All of the periods listed in Table 2 are comfortably in the range of those observed from magnetic CVs, although only 3 such systems are known with periods shorter than that of CXOGC J174517.4–290650,  $P = 321$  s. In contrast, the 68 Galactic HMXB pulsars in the catalog of Liu et al. (2000) have a median  $P \approx 91$  s, and only 3 have  $P > 900$  s. Although this suggests that the sources detected with periodicities at the Galactic center are more likely to be magnetic CVs, it should be emphasized that there is no lower limit to how slowly a wind-accreting neutron star can rotate. Indeed, the slowest pulsar known, 4U 0114+650, has a period of over  $10^4$  s (Hall et al. 2000), which is comparable to the longest periods listed in Table 2.

Finally, our ability to use the seven sources with peri-

odicities to draw conclusions about the entire sample of hard sources at the Galactic center is limited, because the Doppler motion of a neutron star in its binary orbit can prevent us from detecting the short-period modulations that are typical of HMXB pulsars. This Doppler motion would smear the power in a coherent pulsar signal over several adjacent frequency bins. For a circular orbit, the shift in frequency is approximately

$$\frac{\Delta\nu}{\nu} = 1.5 \times 10^{-3} \frac{M_C \sin i}{M_{\text{tot}}^{2/3} P_{\text{day}}^{1/3}} \left( 1 - \cos \left[ \frac{2\pi\Delta T}{P} \right] \right), \quad (3)$$

where  $M_C$  is the mass of the companion star in solar masses,  $i$  is the inclination of the binary,  $M_{\text{tot}}$  is the total mass of the system,  $P_{\text{day}}$  is the orbital period in days, and  $\Delta T$  is the exposure time. For a massive X-ray binary,  $M_C \approx M_{\text{tot}} \approx 10M_{\odot}$ . The orbital period can be shorter than 1 day in supergiant HMXBs, but the more common Be systems tend to have orbital periods between 10–300 days (Liu et al. 2000). For a 10-day orbit, a  $10 M_{\odot}$  companion, and an inclination of  $60^\circ$ , the power from pulsar signals faster than  $\approx 2600$  s would be spread over two frequency bins. Therefore, binary motion easily could explain why we did not detect any signals faster than  $10^{-2}$  Hz, which would be expected from HMXB pulsars.

Thus, the long periods of the seven Galactic center

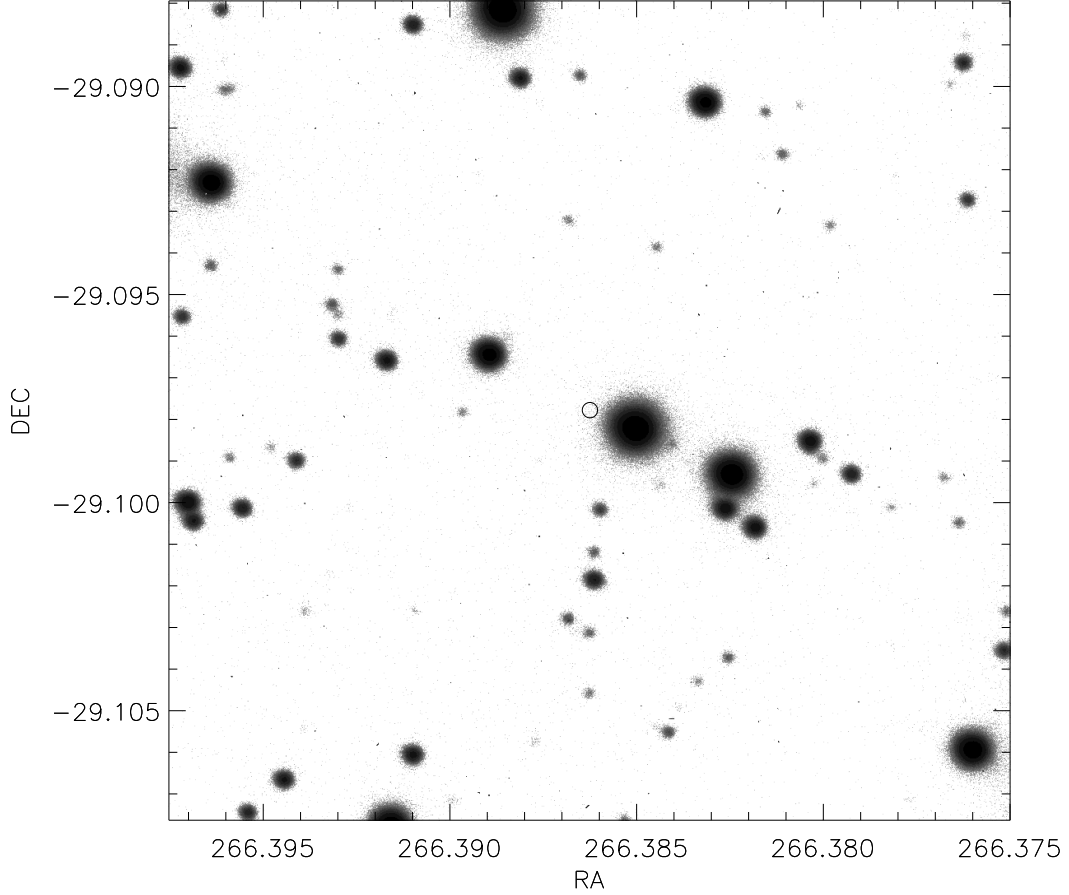


FIG. 6.— Image of the 2.4 arcmin<sup>2</sup> field around CXOGC J174532.7–290552 taken from a 5 min  $i'$  band exposure using MagIC on the Clay telescope (Magellan-II). The 1  $\sigma$  error circle for CXOGC J174532.7–290552 is marked; there is no counterpart down to  $i' \approx 23$  mag.

sources with modulations provide marginal evidence that they are magnetic CVs. However, the possibility that they are HMXB pulsars cannot be ruled out, and the difficulty of detecting short-period modulations from HMXBs prevents us from extrapolating this conclusion to the hundreds of hard sources at the Galactic center for which we have not detected significant periodic variations. Indeed, it seems likely that other sources with periodic variability below our detection threshold are present in the image. In Figure 5, we have indicated with vertical dotted lines the approximate total numbers of counts required to detect sources with 30% and 50% rms sinusoidal modulations. Only the magnetic CVs and HMXB pulsars with the largest-amplitude modulations would have been detectable in our search, which suggests that periodicities could be detected from many of the hard sources in a deeper exposure.

### 3.2. CXOGC J174532.7–290552 = RXJ 1745.5–2905

The foreground source, CXOGC J174532.7–290552, was first identified as the *ROSAT* source RXJ 1745.5–2905 (source 11 in Predehl & Truemper 1995), although an X-ray periodicity has not previously been reported from the source. The folded light curve of CXOGC J174532.7–290552 in Figure 2 exhibits two distinct features that recur with the same period: a gradual,

large-amplitude modulation in the total X-ray flux, and a sharp, 250 s eclipse during which the entire X-ray emitting region is obscured. These features demonstrate that this source is a polar (AM Her-type system), in which the spin period of the white dwarf is synchronized to that of the orbital period. The smooth, large amplitude modulation is produced by the rotation of the white dwarf, which causes the hot region on the white dwarf onto which the accreted material is magnetically channeled to be periodically obscured. The short eclipse occurs because we observe the system along the orbital plane with an inclination  $i > 75^\circ$ , so the companion star occults the much smaller white dwarf (see Warner 1995, for a review).

The absorption column toward the source,  $N_{\text{H}} \approx 5 \times 10^{21} \text{ cm}^{-2}$ , can be used to estimate its distance roughly. If we assume that the density of gas and dust in the Galactic disk is distributed radially as an exponential with a scale length of 2.7 kpc (Kent, Dame, & Fazio 1991) and that its total column to the Galactic center distance of 8 kpc is  $6 \times 10^{22} \text{ cm}^{-2}$  (Baganoff et al. 2003), then we find that CXOGC J174532.7–290552 lies at a distance of  $\approx 2.5$  kpc. This would rank CXOGC J174532.7–290552 with the recently-identified globular cluster CVs (e.g., Grindlay et al. 2001; Pooley et al. 2002; Edmonds et al. 2003) as one of the most distant polars ever identified;

the only CVs otherwise identified at such large distances are classical novae and super-soft X-ray sources (compare Warner 1995). We can infer that its X-ray luminosity is  $\approx 4 \times 10^{30} \text{ erg s}^{-1}$ , which is well within the range commonly observed from polars (Ezuka & Ishida 1999).

Since this source is in the foreground of the Galactic center, we have attempted to identify its optical counterpart. An observation of the field around CXOGC J174532.7–290552 was obtained using the Raymond and Beverly Sackler Magellan Instant Camera (MagIC) on the 6.5 m Clay (Magellan-II) telescope at Las Campanas Observatory in Chile. MagIC is a  $2048 \times 2048$  SITe CCD with a plate scale of  $0''.069 \text{ pixel}^{-1}$  and a field of view of  $2.36 \text{ arcmin}^2$ . MagIC was installed at the west f/11 Nasmyth focus of the telescope. The observation occurred during the first science run on 2002 September 7. The field was exposed for 5 min behind a Sloan  $i'$  filter (Fukugita et al. 1996). The seeing was  $0.8''$  (FWHM). The resulting image, corrected for bias variations between the 4 CCDs, is displayed in Figure 6. Unfortunately, no standard star was observed in the  $i'$  band because of technical problems later in the evening.

No counterpart was found within  $1.5''$  of CXOGC J174532.7–290552 (Figure 6). Without a standard star for calibration, we can only estimate an upper limit of  $i' < 23$  mag for the intensity of CXOGC J174532.7–290552 based on exposures taken with MagIC with similar seeing and duration. The column density of absorbing material toward the source,  $H_{\text{H}} = 5 \times 10^{21} \text{ cm}^{-2}$ , implies a visual reddening of  $A_V = 2.8$  magnitudes (Predhel & Schmitt 1995), which translates to an extinction near the  $i'$  band of  $A_I = 1.3$  magnitudes (Rieke & Lebofsky 1985). Thus, the deabsorbed  $i'$  magnitude of the counterpart is fainter than  $\approx 21$  mag. Its absolute magnitude would then be  $M_{i'} \gtrsim 9$  for a distance of 2.5 kpc.

This limit on the magnitude of the companion is not unreasonably faint for a polar. Eleven polars with orbital periods shorter than 2 h are listed both with optical magnitudes in the catalog of Ritter & Kolb (2003), and with distances in (Warner 1995). We find that the absolute V-band magnitudes of these 11 sources range from 11.3 – 13.7 mag when they are in low optical states, and 7.3 – 9.5 in high optical states. To convert these  $M_V$  magnitudes to  $M_{i'}$  values, we note that the infrared colors of magnetic CVs are similar to M dwarf stars (Hoard et al. 2002), so that  $V - i' \approx 2$  (compare Fukugita et al. 1996; Kilkenny et al. 1998). Thus, we expect that in low optical states these polars would be comparable to or fainter than the lower limit of  $M_{i'} > 9$  mag for CXOGC J174532.7–290552. However, all but one of these same polars (the exception being EP Dra) should be easily observable in their brighter optical states from 2.5 kpc away. Since the X-ray emission from CXOGC J174532.7–290552 clearly exhibits large variations in its X-ray intensity on time scales of a

year (Figure 3), it probably also exhibits significant optical variability (Warner 1995). It is therefore possible that CXOGC J174532.7–290552 was observed in a low optical state in 2002 September.

#### 4. CONCLUSIONS

We have identified eight sources of periodic X-ray variability in 487 ks of observations of the  $17' \times 17'$  field centered on the Galactic center that were taken over a two week span in 2002 May 22 through June 4 (Table 2 and Figure 1). The X-ray spectra of these sources indicate that seven lie near or beyond the Galactic center, while one is in the foreground at a distance of approximately 2.5 kpc (Table 3 and Figure 4). The spectra, luminosities, and periods of the Galactic center sources are all consistent with either magnetized CVs or HMXB pulsars; future infrared observations will be required to determine the exact natures of these sources. The light curve of the foreground source indicates that it is an eclipsing polar. We have searched for an optical counterpart in an  $i'$  image obtained with the Clay (Magellan II) telescope, but none was found down to a deabsorbed  $i'$  magnitude of 21. A polar in a low optical state at 2.5 kpc from Earth would probably have an  $i'$  magnitude that is slightly fainter.

These sources are probably not unique to the Galactic center, as they are similar to a number of sources with hard spectra and X-ray periods longer than 100 s that recently have been identified in the plane of the Galaxy (Kinugasa et al. 1998; Torii et al. 1999; Oosterbroek et al. 1999; Sugizaki et al. 2000; Sakano et al. 2000). However, they are the faintest sources ever observed to show periodicities. The periodic variations were detectable only because *Chandra* observed the Galactic center almost continuously for nearly 500 ks. Unfortunately, unless such long monitoring campaigns are carried out with *Chandra* in the future, the detection of similar periodicities is unlikely. The larger effective areas of future X-ray missions may allow periodicities to be detected from sources using shorter observations. However, current plans for these missions lack the  $< 1''$  angular resolution required to resolve the faint X-ray sources in regions like the Galactic center, where both the density of sources and the flux from diffuse emission are high.

We are grateful to S. Burles for obtaining the optical image of CXOGC J174532.7–290552, and for advising us about how to process the image. We also thank Z. Wang for advice on the optical processing, and M. Eracleous, D. Galloway, and J. Sokoloski for helpful discussions about the possible natures of these sources. We thank the referee, J. Grindlay, for his helpful comments. This work has been supported by NASA grants NAS 8-39073 and NAS 8-00128. W.N.B. also acknowledges the NSF CAREER award AST-9983783.

#### REFERENCES

Apparao, K. M. V. 1994, *SSRev*, 69, 255  
 Baganoff, F. K. et al. 2003, *ApJ*, to appear in v590, n2  
 Broos, P., Townsley, L., Getman, K. & Bauer, F. 2002, “ACIS Extract, An ACIS Point Source Extraction Package”, Pennsylvania State University, <http://www.astro.psu/xray/docs/TARA/ae-users-guide.html>  
 Buccieri, R. et al. 1983, *A&A*, 128, 245  
 Campana, S., Gastaldello, F., Stella, L., Israel, G. L., Colpi, M., Pizzolato, F., Orlandini, M., & Dal Fiume, D. 2001, *ApJ*, 561, 924  
 Edmonds, P. D., Gilliland, R. L., Heinke, C. O. & Grindlay, J. E. 2003, *ApJ* submitted, [astro-ph/0307189](http://arxiv.org/abs/astro-ph/0307189)  
 Ezuka, H. & Ishida, M. 1999, *ApJS*, 120, 277

Fukugita, M., Ichikawa, T., Gunn, J. E., Doi, M., Shimasaku, K., & Schneider, D. P. 1996, AJ, 111, 1748

Garmire, G. P., Bautz, M. W., Ford, P. G., Nousek, J. A., & Ricker, G. R. 2002, SPIE Vol. 4851, "Advanced CCD Imaging Spectrometer (ACIS) Instrument on the *Chandra* X-ray Observatory"

Gehrels, N. 1986, ApJ, 303, 336

Grindlay, J. E., Heinke, C., Edmonds, P. D. & Murray, S. S. 2001, Science, 292, 2290

Haberl, F., Angelini, L., Motch, C., & White, N. E. 1998, A&A, 330, 189

Hall, T. A., Finley, J. P. Corbet, R. H. D., & Thomas, R. C. 2000, ApJ, 536, 450

Hellier, C., Mukai, K., & Osborne, J. P. 1998, MNRAS, 297, 526

Hoard, D. W., Wachter, S., Clark, L. L., & Bowers, T. P. 2002, ApJ, 569, 1037

Howell, S. B., Nelson, L. A., & Rappaport, S. 2001, ApJ, 550, 897

Iben, I. Jr., Tutukov, A. V., & Fedorova, A. V. 1997, ApJ, 486, 955

Israel, G. L. et al. 2000, MNRAS, 314, 87

Kalogera, V. 1999, ApJ, 521, 723

Kent, S. M., Dame, T. M., & Fazio, G. 1991, ApJ, 378, 131

Kilkenny, D., van Wyk, F., Roberts, G., Marang, F., & Cooper, D. 1998, MNRAS, 294, 93x

Kinugasa, K. et al. 1998, ApJ, 495, 435

Leahy, D. A., Darbro, W., Elsner, R. F., Weisskopf, M. C., Sutherland, P. G., Kahn, S., & Grindlay, J. E. 1983, ApJ, 266, 160

Liu, Q. Z., van Paradijs, J., & van den Heuvel, E. P. J. 2000, A&AS, 147, 25

Morris, M. 1993, ApJ, 408, 496

Muno, M. P., Baganoff, F. K., Bautz, M. W., Ricker, G. R., Morris, M., Garmire, G. P., Feigelson, E. D., Brandt, W. N., Townsley, L. K., & Broos, P. S. 2003, ApJ, 589, 225

Negueruela, I., Reig, P., Finger, M. H., & Roche, P. 2000, A&A, 356, 1003

Norton, A. J. & Watson, M. G. 1989, MNRAS, 237, 853

Oosterbroek, T., Orlandini, M., Parmar, A. N., Angelini, L., Israel, G. L., Dal Fiume, D., Mereghetti, S., Santangelo, A., & Cusumano, G. 1999, A&A, 351, L33

Pfahl, E., Rappaport, S., & Podsiadlowski, P. 2002, ApJ, 571, L37

Podsiadlowski, P., Rappaport, S., & Pfahl, E. D. 2002, ApJ, 565, 1107

Pooley, D. et al. 2002, ApJ, 569, 405

Predel, P. & Schmitt, J. H. M. M. 1995, A&A, 293, 889

Predel, P. & Truemper, J. 1994, A&A, 290, L29

Press, W. H., Flannery, B. P., Teukolsky, S. A., & Vetterling, W. T. 1992, Numerical Recipes in C, 2nd Ed. (Cambridge: Cambridge University Press)

Ramsay, G. & Cropper, M. 2003, MNRAS, 338, 219

Rappaport, S. & van den Heuvel, E. P. J. 1982, IAU Symposium, 98, 327

Reig, P. & Roche, P. 1999, MNRAS, 306, 100

Rieke, G. H. & Lebofsky, M. J. 1985, ApJ, 288, 618

Ritter, H. & Kolb, U. 2003, to appear in A&A, astro-ph/0301444

Sakano, M., Torii, K., Koyama, K., Maeda, Y., & Yamauchi, S. 2000, PASJ, 52, 1141

Schwarz, R., Greiner, J., Tovmassian, G. H., Zharikov, S. V., & Wenzel, W. 2002, A&A, 392, 505

Serabyn, E. & Morris, M. 1996, Nature, 382, 602

Sugizaki, M., Kinugasa, K., Matsuzaki, K., Terada, Y., Yamauchi, S., & Yokogawa, J. 2000, ApJ, 534, L181

Torii, K., Sugizaki, M., Kohmura, T., Endo, T., & Nagase, F. 1999, ApJ, 523, L65

Townsley, L. K., Broos, P. S., Garmire, G. P., & Nousek, J. A. 2000, ApJ, 534, L139

Vaughan, B. A. et al. 1994, ApJ, 435, 362

Verbiest, F., Bunk, W. H., Ritter, H., & Pfeffermann, E. 1997, A&A, 327, 602

Warner, B. 1995, *Cataclysmic Variable Stars*, Cambridge University Press

White, N. E., Nagase, F., & Parmar, A. N. (1995). In Lewin, W. H. G. and van Paradijs, J. and van den Heuvel, E. P. J., editor, *X-ray Binaries*, Cambridge University Press, pg. 1

TABLE 1  
OBSERVATIONS OF THE INNER 20 PC OF THE GALAXY

No.	Start Time (UT)	ObsID	Exposure (s)	Aim Point		
				RA (degrees J2000)	DEC (degrees J2000)	Roll (degrees)
1	1999 Sep 21 02:43:00	0242	40,872	266.41382	-29.0130	268
2	2000 Oct 26 18:15:11	1561	35,705	266.41344	-29.0128	265
3	2001 Jul 14 01:51:10	1561	13,504	266.41344	-29.0128	265
4	2002 Feb 19 14:27:32	2951	12,370	266.41867	-29.0033	91
5	2002 Mar 23 12:25:04	2952	11,859	266.41897	-29.0034	88
6	2002 Apr 19 10:39:01	2953	11,632	266.41923	-29.0034	85
7	2002 May 07 09:25:07	2954	12,455	266.41938	-29.0037	82
8	2002 May 22 22:59:15	2943 <sup>a</sup>	34,651	266.41991	-29.0041	76
9	2002 May 24 11:50:13	3663 <sup>a</sup>	37,959	266.41993	-29.0041	76
10	2002 May 25 15:16:03	3392 <sup>a</sup>	166,690	266.41992	-29.0041	76
11	2002 May 28 05:34:44	3393 <sup>a</sup>	158,026	266.41992	-29.0041	76
12	2002 Jun 03 01:24:37	3665 <sup>a</sup>	89,928	266.41992	-29.0041	76

<sup>a</sup>These observations were used to search for sources with periodic variability.

TABLE 2  
SOURCES WITH PERIODIC X-RAY VARIATIONS

Name (CXOGC J)	$N_{\text{tot}}$ (counts)	$B$	$P$ (s)	$A$ (rms %)	$T_0^{\text{a}}$ (MJD [TDB])
174517.4–290650	273 <sup>b</sup>	53.6	321.51(5)	55(8)	52416.9585(2)
174531.7–290542	233	67.6	16772(16)	60(9)	52416.981(7)
174532.3–290251	304	24.5	5612(2)	58(6)	52416.977(2)
174532.7–290552	1260	64.1	5409.6(6)	71(2)	52416.9409(7)
174534.5–290201	724	31.3	971.64(5)	40(4)	52416.9595(3)
174535.6–290034	466	70.3	9907(8)	49(5)	52417.011(4)
174541.8–290037	493	138.6	1092.15(6)	53(6)	52416.9546(4)
174543.4–285841	410	40.8	5313(2)	48(6)	52416.953(2)

<sup>a</sup>Defined by zero phase when fitting a sinusoid to the fundamental frequency.

<sup>b</sup>Only data from ObsIDs 2943 and 3663 were used for this source, as it later declined in flux and the pulsations disappeared.

Note. —  $1\sigma$  uncertainties on the last significant digit are indicated in parenthesis.

TABLE 3  
X-RAY SPECTRA OF SOURCES WITH PERIODICITIES

Name (CXOGC J)	Flux	$N_{\text{H}}$	$\Gamma$	$E_{\text{Fe}}$	$W_{\text{Fe}}$	$N_{\text{Fe}}$	EW	$\chi^2/\nu$
174517.4–290650	4.4	$6^{+7}_{-2}$	$1.0^{+1.7}_{-0.7}$	$6.6^{+0.1}_{-0.1}$	$0.2^{+0.1}_{-0.1}$	$0.9^{+0.4}_{-0.4}$	960	63/42
174531.7–290542	1.7	$9^{+9}_{-7}$	$-0.6^{+1.6}_{-1.3}$	...	...	...	...	13/11
174532.3–290251	2.8	$25^{+9}_{-10}$	$1.8^{+1.5}_{-1.2}$	$6.66^{+0.04}_{-0.03}$	$< 0.2$	$0.8^{+0.5}_{-0.3}$	640	15/15
174532.7–290552	3.2 <sup>a</sup>	$0.5^{+0.1}_{-0.1}$	$1.4^{+0.1}_{-0.1}$	...	...	...	...	59/61
174534.5–290201	6.8	$13^{+8}_{-3}$	$0.5^{+1.4}_{-0.5}$	$6.6^{+0.2}_{-0.1}$	$0.3^{+0.1}_{-0.1}$	$1.7^{+1.4}_{-0.6}$	720	30/40
174535.6–290034	3.3	$13^{+5}_{-4}$	$0.9^{+0.9}_{-0.8}$	...	...	...	...	25/25
174541.8–290037	4.6	$12^{+14}_{-7}$	$0.3^{+1.0}_{-1.2}$	$6.6^{+0.1}_{-0.1}$	$0.13^{+0.11}_{-0.09}$	$1.2^{+1.1}_{-0.4}$	920	28/28
174543.4–285841	4.0	$15^{+10}_{-3}$	$0.6^{+1.4}_{-0.3}$	...	...	...	...	26/22

<sup>a</sup>The 0.5–8 keV flux for this foreground source was  $3.7 \times 10^{-14}$  erg cm $^{-2}$  s $^{-1}$ .

Note. — The flux is in units of  $10^{-14}$  erg cm $^{-2}$  s $^{-1}$  (2–8 keV). The column density  $N_{\text{H}}$  is in units of  $10^{22}$  cm $^{-2}$ .  $\Gamma$  is the photon index. The energy  $E_{\text{Fe}}$  and width  $W_{\text{Fe}}$  of the line emission are in keV, and the flux in the line  $N_{\text{Fe}}$  is in units of  $10^{-6}$  photons cm $^{-2}$  s $^{-1}$ . The equivalent width is in units of eV. Uncertainties are 90% confidence ranges for one parameter of interest.